Journal of Inclusion Phenomena and Macrocyclic Chemistry **36:** 79–93, 2000.

The Stability of Self-inclusion Complexes of Cyclodextrin Derivatives Bearing a *p*-Dimethylaminobenze Moiety

TETSUYA TANABE, SHINJI USUI, ASAO NAKAMURA and AKIHIKO UENO*

Faculty of Bioscience and Biotechnology, Tokyo Institute of Technology, 4259 Nagatsuta-cho, Midori-ku, Yokohama 226-8501, Japan

(Received: 16 October 1998; in final form: 11 March 1999)

Abstract. An appending moiety of modified cyclodextrins acts as an intramolecular guest and forms a self-inclusion complex in aqueous solution. In this study, the stability of self-inclusion complexes of modified cyclodextrins which have a *p*-dimethylaminobenzene moiety was analyzed by fluorescent decay analyses, and the factor that determines the stability of the self-inclusion complex was determined by a computational approach. The self-inclusion form is stabilized mainly due to van der Waals interaction between the appending moiety and the cyclodextrin ring.

Key words: modified cyclodextrin, inclusion complex, fluorescence, molecular mechanics

1. Introduction

Cyclodextrins (CDs) are cyclic oligomers which have $\alpha 1 \rightarrow 4$ linked D-glucose units. CDs consisting of six, seven, and eight glucose units are most popular and named as α-, β-, and γ-CD, respectively. They have the remarkable property of including various organic molecules in their central cavity in aqueous solution, and a large number of papers discussing the stability of the inclusion complexes have been published [1]. On the other hand, modified CDs, which have a functional residue attached at the secondary or primary hydroxyl side, have been synthesized as sensors of molecular recognition or enzyme-mimetic catalyses. In such CDs, the typical appending moieties are fluorophors or catalytic moieties. Interestingly, Ueno and co-workers indicated that many appending moieties of modified CDs tend to be included in the CD cavity, forming self-inclusion complexes [2–4]. However the stability of the self-inclusion complexes has not been discussed until now. In this paper, the stability of self-inclusion complexes will be discussed in detail on two modified cyclodextrins bearing the *p*-dimethylaminobenze moiety as the primary hydroxyl side. One of the modified CDs is 6-deoxy-(6-*p*-dimethylaminobenzoyl)-amino-β-CD (DMAB-β-CD, see Figure 1(a)) and the

* Author for correspondence.

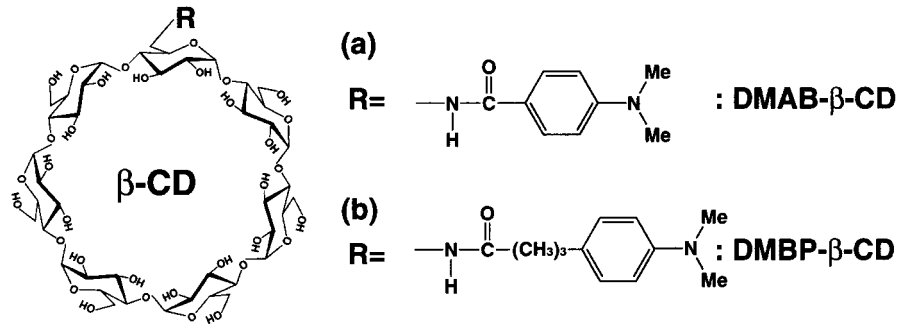

Figure 1. The structure of DMAB-β-CD (a) and DMBP-β-CD (b).

other is 6-deoxy-(6-*p*-dimethylaminobenzene butyryl)-amino-β-CD (DMBP-β-CD, see Figure 1(b)). The conformation of DMAB-β-CD was analyzed by induced circular dichroism spectra, fluorescence spectra, and ^{1}H-NMR spectra previously [5] and it was found that DMAB-β-CD takes a self-inclusion form in aqueous solution although there exists an equilibrium between two forms with the appending moiety inside (form A) and outside (form B) of the CD cavity (schematic images of A and B forms are shown in Figure 2). Furthermore it was estimated by CPK model analysis that the formation of the self-inclusion complex is rather difficult for DMAB-β-CD because of the limited ability of the DMAB moiety to be included in DMAB-β-CD. On this basis, it is interesting to examine the stability of self-inclusion complexes on the modified CDs with and without a flexible appending moiety. From this viewpoint, DMBP-β-CD, which has trimethylene units between the CD and the DMAB moiety, was synthesized for comparison, and the stability of the self-inclusion complexes of DMBP-β-CD and DMAB-β-CD was examined. Analysis by the molecular dynamics and molecular mechanics calculation on the formation of self-inclusion complexes was performed in this study. These results provide interesting information on the conformation of modified CDs and may be a useful guide for constructing new functional modified CDs.

2. Method

The DMBP-β-CD was prepared by the reaction of 6-deoxy-6-amino-β-cyclodextrin with 4-(4-dimethylaminophenyl)butyric acid. The conformational analysis was performed as described for DMAB-β-CD. The stability of the self-inclusion complexes were measured by fluorescence decay analysis.

3. Experimental

β-cyclodextrin was kindly donated by Nihon Shokuhin Kako Co., Ltd. All other reagents were purchased from a chemical supplier and used without further puri-

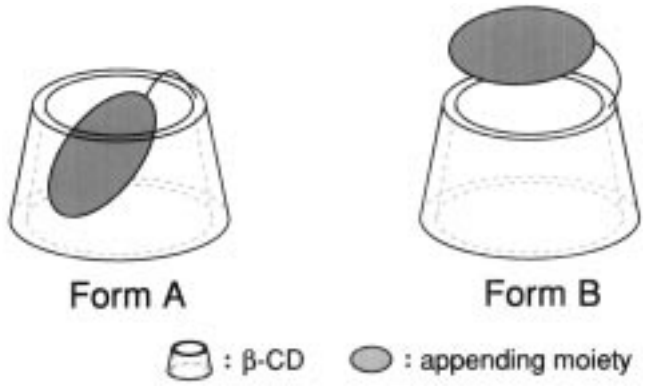

Figure 2. Schematic representation of typical conformations of modified CDs.

fication. The water used for photometry and deuterium oxide used for the NMR study were obtained from Cica-Merck and Merck, respectively.

Absorbance, fluorescence, and circular dichroism spectra were measured on a Shimazu UV3100 spectrophotometer, HITACHI 850 fluorescence spectrometer, and a JASCO J-600 spectropolarimeter or a JASCO J720WI spectropolarimeter. ^{1}H-NMR spectra were measured on a Varian VXR 500S spectrometer (500 MHz). Time of flight mass spectra (TOF-MASS) were measured on a Shimazu KRATOS KOMPACT MALDII III mass spectrometer with gentisic acid as the matrix. Fluorescence decay was measured by a time-correlated single proton counting method on a Horiba NAES-550 system. A self-oscillation flash lamp filled with H_2 was used as a light source. The excitation beam passed through FS300-10 (DMAB-β-CD and DMBP-β-CD), and the emission beam was passed through the filter UV-34 (for DMAB-β-CD) and L370 (for DMAB-β-CD). The excitation wave lengths for both DMAB-β-CD and DMBP-β-CD were 300 nm. Thin-layer chromatography (TLC, butanol/ethanol/water/ = 5 : 4 : 3) was carried out with silica gel 60 F_{254} (Merck Co.).

3.1. SYNTHESIS

3.1.1. *4-(4-Dimethylaminophenyl)butyric Acid*

Esterification. 4-(4-nitrophenyl)butyric acid (2.0 g) was suspended in EtOH and conc. H_2SO_4 added (1 drop). The mixture was heated (60 °C) under reflex for 4.5 h, evaporated to remove EtOH and ethyl acetate, ice, and $NaHCO_3$ were added. The ethyl acetate solution was separated by a separatory funnel (three times), washed with aqueous NaCl solution and dried over $MgSO_4$ (two times). After ethyl acetate was removed by evaporation, oily 4-(4-nitrophenyl)butyric ethyl ester was obtained. Silica gel column chromatography with a mixed solution of two solvents (hexane: acetic ethyl ester = 1 : 1) yielded a yellowish oil (1.92 g, yield 84.7%).

Alkylation (Synthesis of 4-(4-Dimethylaminophenyl)butyric Ethyl Ester). In a 400 ml autoclave were placed 4-(4-nitrophenyl)butyric acid ethyl ester (1.92 g), ethanol (10.5 ml), 35% aqueous formaldehyde solution (2.4 ml) and palladium on charcoal (0.105 g). The sample was filled with argon (two times), and then filled with hydrogen (three times, 7.2 atm). The reaction was performed with stirring at room temperature (2.5 h). When the pressure dropped to 5.0 atm, the hydrogen was refilled (7.2 atm). After the pressure dropped to 2.5 atm, the hydrogen was vented from the autoclave and the ethanol solution was filtered. The ethanol was removed by evaporation, and the residue was washed with diethyl ether. The removal of diethyl ether afforded the crude product. The purification was carried out by silica gel column chromatography with a mixed solvent (hexane: acetic ethyl ester = 3 : 1), yielding the yellowish oil (800 mg, yield 41.1%). The purity was checked by ^{1}H-NMR, (D_2O 500 MHz): δ 1.25 (t, 3H, —CH_3), δ 1.95 (quintet, 2H, —CH_2-), δ 2.25 (t, 2H, —CH_2—), δ 2.55 (t, 2H, —CH_2—), δ 2.92 (s, 6H, —$N(Me)_2$), δ 4.15 (t, 2H, —CH_2—), δ 6.55 (d, 2H, aromatic), δ 7.05 (d, 2H, aromatic), and TLC.

Hydrolysis. 4-(4-Dimethylaminophenyl)butyric ethyl ester (722 mg) was suspended in water (10 ml) and HClaq added (three $\sim$ four drops). The solution was heated and the reaction carried out under reflux for 1.5 h. The solution was extracted by ethyl acetate two times and evaporation of ethyl acetate afforded the crude product. The purification was carried out by silica gel column chromatography with a mixed solution of solvents (hexane: acetic ethyl ester = 1 : 1) and purity was checked by ^{1}H-NMR, (D_2O 500 MHz): δ 1.94 (quintet, 2H, —CH_2—), δ 1.95 (t, 2H, —CH_2—), δ 2.64 (t, 2H, —CH_2—), δ 3.10 (s, 6H, —$N(Me)_2$), δ 7.20 (d, 2H aromatic), δ 7.24 (d, 2H, aromatic), and TLC (500 mg 78.4%).

3.1.2. *Mono-6-deoxy-6-(4-(4-dimethylaminophenyl)propyl)-amide-β-CD, (DMBP-β-CD)*

NH_2-β-CD (1.6 g) was suspended in N-methylpyroltdone (30 ml) and cooled below 0 °C. 4-(4-dimethylaminophenyl)butyric acid (0.12 g), dicyclohexylcarbodiimide (DCC, 0.1 g), and 1-hydroxybenzotriazol (HOBt, 0.082 g) were added to the solution with stirring and reacted for 162 h. Then, the solution was poured into acetone (500 ml), and the formed precipitate was dried in vacuum overnight, giving 0.19 g of crude product. The crude product was purified by repeated recrystallization (solvent, H_2O), giving white powder (0.088 g, R_f = 0.50, yield 13.6%). Anal. Calcd for $C_{54}H_{86}O_{35}N_2 \cdot 5H_2O$: C, 45.48; H, 6.78; O, 44.87; N, 1.96. Found C, 45.62; H, 6.51; N, 1.89. ^{1}H-NMR (DMSO-d_6 500 MHz): δ 1.68 (t, 2H, —CH_2—), δ 2.08 (m, 2H, —CH_2—), δ 2.40 (t, 2H, —CH_2—), δ 2.81 (s, 6H, —$N(Me)_2$), δ 3.0 $\sim$ 4.8 (m, H2, H3, H4, H5, H6 protons of β-CD moiety) , δ 4.9 (m, H1 protons of β-CD moiety), δ 6.62 (d, 2H aromatic), δ 6.98 (d, 2H, aromatic). The TOF-MASS spectrum had peaks at 1347 (M + 23) units.

3.2. MOLECULAR DYNAMICS CONFORMATIONAL SEARCH

Model building of the initial starting conformations of DMAB-β-CD and DMBP-β-CD were performed with the aid of interactive molecular graphics. Two types of initial conformations were prepared for DMAB-β-CD and DMBP-β-CD. The first one is the conformation with the appending moiety included in its CD cavity (form A) and second one is that with the appending moiety located out of the CD cavity (form B). In order to obtain the partial atomic charges for appending moieties the AM1 hamiltonian of Ampac ver. 2.10 was used. The charges for the CD ring were obtained from parameterized sets with consistent valence force field (CVFF). All parameters were used as implemented in the generic parameter set of CVFF. The initial conformation of the two compounds were subjected to energy minimization with the aid of CVFF until the maximum derivative became less than 0.5 kcal/mol. Starting with the minimized conformations, MD at 500 K was carried out for 200 ps after an initial 10 ps equilibration time. An integration step of 1 femto second was used. During the calculation, a structure is stored every 1 ps and subsequently energy is minimized until the maximum derivatives became less than 0.01 kcal/mol. To maintain the structure of the pyranose ring in the $^4C_1$ form, during the MD calculation, the torsion angles, which were included in the pyranose rings, were constrained to the initial values by adding a harmonic forcing at a constant of 20 kcal/mol. But this restriction was removed in the potential minimization. There was no cut-off radius for the nonbond interaction. A distance(r)-dependent dielectric constant of 2.5r was used. These procedures of calculation were applied to two compounds with initial structure of the A and B forms. During the 200 ps MD conformational search no conformational change between the A and B forms occurred for DMAB-β-CD, so the 200 minimized structures with the A and B forms were obtained, starting from A and B forms as initial structure, respectively. The conformations, which were obtained from the MD conformational search, were stored with the values of the total energies and 50 stable structures were used for the analyses for the A and B forms, respectively. A similar methodology employed for DMAB-β-CD was used to search the conformation of the DMBP-β-CD, however the appending moieties of the DMBP-β-CD compounds were so flexible that the appending moieties were unsteady during the MD conformational search, i.e., the conformational change between the A and B forms occurred easily during the simulations irrespective of the initial structure of the A and B forms. Therefore one can obtain stable structures of both the A and B forms by one simulation. From the 200 minimized conformations obtained from the MD conformational search provided both structures taking A and B forms and they were divided into A and B forms for analyses. The definition of the A and B forms was as follows: the conformations with the phenyl moiety vertically included in the CD cavity (a distance less than 1 Å between the center of the benzene rings and the center of the CD moiety) were defined as form A. Only fifty structures which had lower potential energies than others were taken into account for the data analyses. The

B form was defined for the conformations which did not satisfy the definition of form A, and a lot of conformations existed in the minimized structure for form B, so we could not characterize it. When the conformations were rearranged by the order of potential energies, it was found that all fifty structures, which had lower potential energies than others, took the conformation with the appending moiety near the primary hydroxyl side of β-CD, so these structures were assigned to form B. As a result the 50 structures for the A and B forms of DMBP-β-CD were used for data analyses. All calculations were performed on a Silicon Graphic Personal Iris 4D/35 or Indigo2 workstation. For model building and MD calculations, the programs InsightII ver. 2.30 or ver. 95.0 and Discover ver. 2.90 or 95.0 from MSI, Inc., were used.

4. Results and Discussions

4.1. CONFORMATIONAL ANALYSIS OF DMBP-β-CD

4.1.1. *Fluorescence Spectrum*

Figure 3 shows the fluorescence spectra of DMAB-β-CD in 2.5% DMSO aqueous solution (5.0×10^{-5} M). The excitation wavelength was 300 nm. The fluorescence intensity decreased upon addition of 1-adamantanol. Usually, the fluorescence intensity is enhanced when the fluorophore locates in the hydrophobic environment inside of the CD cavity, while the intensity is depressed when it locates in the aqueous environment. The guest-induced fluorescence decrease suggests that the DMBP moiety was excluded from the hydrophobic CD cavity to the bulk water environment associated with accommodation of the guest. In other words, DMBP-β-CD forms a self-inclusion complex in the absence of the guest compound. A schematic image of the guest induced conformational change is shown in Figure 4.

4.1.2. *Circular Dichroism Spectrum*

Figure 5 shows the induced circular dichroism (ICD) spectra of DMBP-β-CD in 2.5% DMSO aqueous solution (5.0×10^{-5} M), alone and in the presence of 1-adamantanol. In the absence of 1-adamantanol a simple positive band was observed for DMBP-β-CD in the 230 to 270 nm region, however the positive peak decreased upon addition of 1-adamantanol and the dichroism intensity was enhanced in the region of 270 nm to 360 nm. The conformational change, which excludes the DMAB moiety from inside to outside of the CD cavity associated with guest accommodation, may be reflected in this spectral change.

4.1.3. ^{1}*H-NMR Spectrum*

The conformation of DMBP-β-CD was also analyzed by ^{1}H-NMR spectroscopy. The nuclear Overhauser effect can be used for detecting two protons which are located closely. In this study the ROESY spectra [6, 7] (rotating frame Overhauser

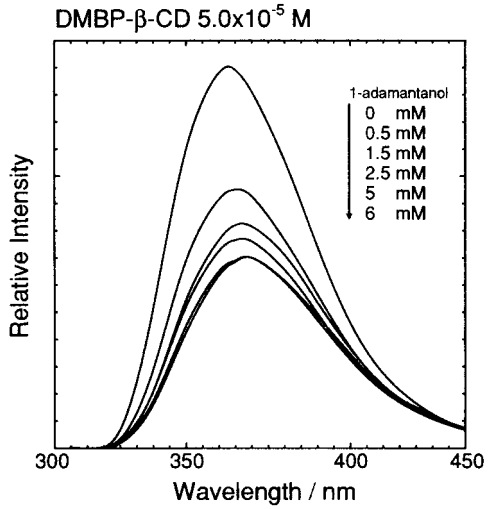

Figure 3. The fluorescence spectra of DMBP-β-CD in 2.5% DMSO aqueous solutions (5.0×10^{-5} M) alone and in the presence of various concentrations of 1-admantanol; excitation wavelength was 300 nm.

Figure 4. Schematic representation of guest induced conformational change of modified CDs.

enhancement spectroscopy) were measured for the DMBP-β-CD. Figure 6 shows the ROESY spectra of DMBP-β-CD (2×10^{-3} M) in DMSO-d_6 2.5% aqueous solution at 25 °C with mixing time of 300 ms (the notation of DMBP-β-CD is also shown in Figure 6). The cross peaks in the region 6.8–7.0 ppm/3.2–4.0 ppm are assigned as the cross peaks between the Hb and Hc protons in the phenyl group and the pyranose protons ($H_2 \sim H_6$ and $H'_2 \sim H'_6$) in CD. And the cross peaks in the region 3.5–4.0 ppm/2.8–3.0 ppm are assigned as the cross peaks between Ha (the protons in the dimethylamino group) and the pyranose protons of CD ($H_1 \sim H_5$). The 1D spectrum of the pyranose region of CD (3.2 to 4.0 ppm) is too complex to assign so we cannot determine which protons in the pyranose ring have cross peaks to the dimethylaminobenzyl group. However the fact that these cross peaks completely disappeared in the presence of 1-adamantanol (1×10^{-3} M) indicates that the observed cross peaks should be assigned as the cross peaks between the protons located inside or on the edge of the CD cavity (H_3, H_5, H_6) and those of the dimethylaminobezene moiety included in the CD cavity.

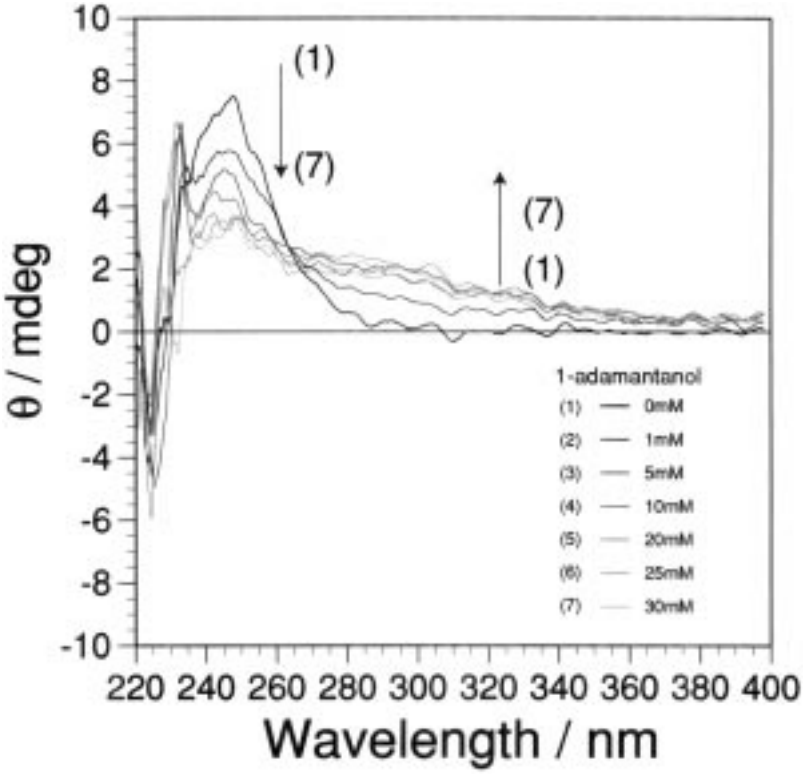

Figure 5. Induced circular dichroism spectra of DMBP-β-CD (5.0×10^{-5} M) in 2.5% DMSO aqueous solution, alone and in the presence of various concentrations of 1-adamantanol.

4.2. THE STABILITY OF THE SELF-INCLUSION COMPLEXES OF DMAB-β-CD AND DMBP-β-CD

4.2.1. *Fluorescence Lifetime*

All conformational analyses of DMBP-β-CD suggest that DMBP-β-CD forms a self-inclusion complex in aqueous solution. In the case of DMAB-β-CD, it was previously reported to form a self-inclusion complex in aqueous solution. These results imply that the two modified CDs take a similar conformation in aqueous solution, however one can predict that the stability of the self-inclusion complexes is different between the two modified CDs on the basis that there exists a flexible methylene chain between the DMAB moiety and the CD residue for DMBP-β-CD, contrasting with the absence of such a chain for DMAB-β-CD. Here the stability of the self-inclusion complex of the two modified CDs will be discussed using fluorescence decay analysis.

Although the conformational interconversion occurs too rapidly to be followed by other spectroscopic methods, the analysis of fluorescence decay of the pendant fluorophore may provide useful information with respect to conforma-

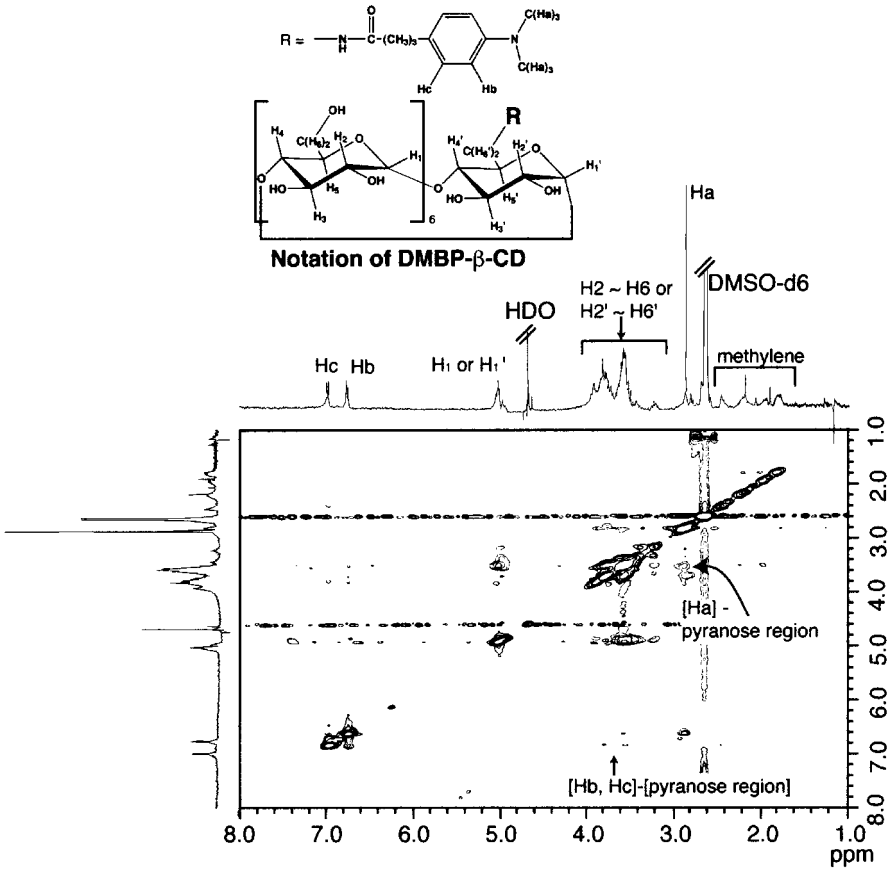

Figure 6. The ROESY spectrum for DMBP-β-CD (2×10^{-3} M) in 25% DMSO aqueous solution, alone and in the presence of guest compound. The notation of DMBP-β-CD is also shown.

tional features since fluorescence lifetimes of many fluorophores are in the range of measurable time scale (nanosecond) for different conformations in an equilibrium. Two aspects of this analysis are (1) to measure the population of the A and B forms in the equilibrium state in aqueous solution, and (2) to measure the enthalpy difference between the A and B forms.

In aqueous solution, the pendant groups of modified cyclodextrins are movable and not fixed in many cases, usually being located either inside the CD cavity (form A) or outside the cavity (form B). The conformational ratio between the A and B forms could be analyzed by the measurements of fluorescence lifetimes of the fluorescent pendant. The analysis of the fluorescence decay usually give different lifetimes for the A and B forms because the fluorescent lifetime is sensitive to the environment [8–10].

Table I. Fluorescence lifetimes of DMAB-β-CD at various temperatures

Temp. (°C)	A_1	A_2	τ_1 (ns)	τ_2 (ns)	K[a]	ΔG[b]
3	0.632	0.368	2.4	1.1	1.72	−0.307
10	0.636	0.364	2.3	1.2	1.75	−0.324
25	0.610	0.390	1.9	1.2	1.56	−0.273
40	0.602	0.398	1.9	0.9	1.51	−0.265

[a] Equilibrium constant between A and B forms calculated from: $K = A_1/A_2$.
[b] Gibbs free energy (kcal mol^{-1}), $\Delta G = -RT \ln K$. R: gas constant, T: absolute temperature.

The fluorescence decay of each modified CD could be analyzed by a simple double exponential function as shown below.

$$I(t) = A_1 \exp(-t/\tau_1) + A_2 \exp(-t/\tau_2)$$

where A_1 is the fraction of form A, A_2 is the fraction of form B, τ_1 is the fluorescence lifetime of form A, τ_2 is the fluorescence lifetime of form B.

DMAB-β-CD exhibits emissions from the nonpolar (NP) and twisted intramolecular charge transfer (TICT) excited state [5], however the fraction of fluorescence decay for the TICT emission, which has a longer lifetime than NP emission, was less than 0.01 in the emission wavelength region (340 nm∼), so we neglected the fraction of TICT emission for the conformational analysis i.e., we assumed that the NP emission may represent the conformational behavior of DMAB-β-CD. The fluorescence decays are summarized in Table I and Table II, for DMAB-β-CD and DMBP-β-CD, respectively. The fraction of the longer lifetime was decreased in the presence of guest (1-adamatanol), therefore the longer (τ_1) and shorter (τ_2) lifetimes species may be ones with the pendant moiety inside (form A) and outside (form B) of the CD cavity. When the populations of the A and B forms are represented by the fractions A_1 and A_2, respectively, the analysis of the decay give the data as shown by A_1:A_2 = 0.610:0.390 and A_1:A_2 = 0.875: 0.125, for DMAB-β-CD and DMBP-β-CD at 25 °C, respectively. This result implies that the population of the self-inclusion complex is ca. 60% and 90%, for DMAB-β-CD and DMBP-β-CD, respectively. On this basis it was clearly demonstrated that the DMBP-β-CD has a larger population of form A than that of DMAB-β-CD.

4.2.2. *Computational Analysis*

The computational approach was applied to the conformational analyses of DMAB-β-CD and DMBP-β-CD. Molecular mechanics (MM) calculations have been widely used on studies of molecular structure and conformational energies [11], so in this study the potential energies of the A and B forms were calculated

Table II. Fluorescence lifetimes of DMBP-β-CD at various temperatures

Temp. (°C)	A_1	A_2	τ_1 (ns)	τ_2 (ns)	K[a]	ΔG[b]
25	0.875	0.125	3.4	2.8	7.00	−1.15
40	0.847	0.153	3.1	2.0	5.54	−1.06
50	0.828	0.172	2.9	1.4	4.81	−1.01
60	0.851	0.149	2.6	1.0	5.71	−1.15
70	0.806	0.194	2.3	0.6	4.15	−0.97
80	0.807	0.193	2.1	0.7	4.18	−1.00

[a] Equilibrium constant between the A and B forms calculated from: $K = A_1/A_2$.
[b] Gibbs free energy (kcal mol^{-1}), $\Delta G = -RT \ln K$. R: gas constant, T: absolute temperature.

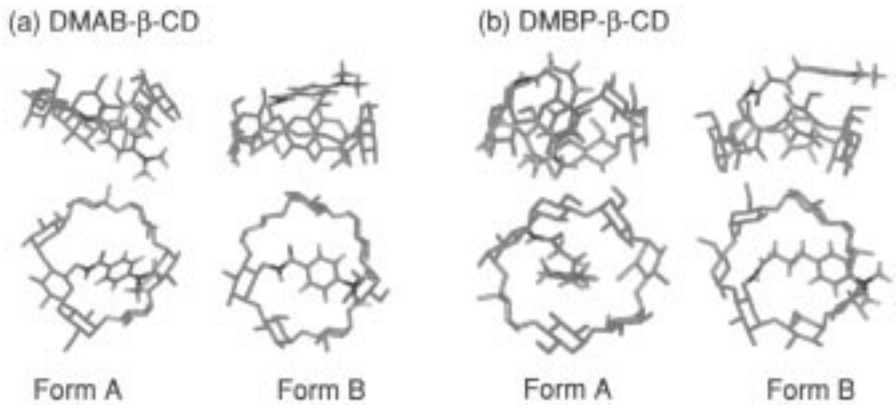

Figure 7. The typical structures of DMAB-β-CD and DMBP-β-CD calculated from MD conformational searches (side view (TOP) and vertical view (BOTTOM)).

by the MM calculations and the total energies were investigated. However we know that simple gradient energy minimization of one initial structure would not be adequate for sampling correct conformational spaces. So we have explored the energy surface of DMAB-β-CD and DMBP-β-CD in a random way using a molecular dynamics (MD) conformational search [15]. The conformations provided by the MD conformational search were divided into A and B forms, furthermore the 50 conformations bearing lower total energies were collected for data analysis (see experimental section for detail). The CVFF force field, which was used in these calculations, has the following form.

$$E_{\text{pot}} = \underset{(1)}{\sum_b D_b(b-b_0)^2} + \underset{(2)}{\sum_\theta H_\theta(\theta-\theta_0)^2} + \underset{(3)}{\sum_\phi H_\phi(1+s\cos(n\phi))}$$

$$+ \underset{(4)}{\sum_\chi H_\chi \chi^2} + \underset{(5)}{\sum \varepsilon\left[\left(\frac{r^*}{r}\right)^{12} - 2\left(\frac{r^*}{r}\right)^{6}\right]} + \underset{(6)}{\sum \frac{q_i q_j}{\varepsilon r_{ij}}}$$

Terms (1) $\sim$ (4) represent the energy deformation of bond length, bond angle, torsion angle, and out-of-plane interaction, respectively and terms (5) and (6) describe non bond interactions, term (5) representing the van der Waals interaction with Lennard–Jones function, and term (6) is the Coulombic representation of electrostatic interaction. It is very difficult to know how the energy hypersurface of a molecule will be changed when the solvent water exists, so the calculations in this study were carried out under pseudo vacuum conditions, using the distance-dependent-dielectric condition to compensate for the lack of explicit water.

The calculated potential energies of the A and B forms are shown in Figure 8(a) and Figure 9(a) for DMAB-β-CD and DMBP-β-CD, respectively, together with the van der Waals (b) and the angle bending (c) energy (the structure number is defined by the order of the total potential energies). There are small variations of other terms of the CVFF function (bond, torsion, out-of-plane, and coulombic terms) so they are not shown in the figure. It was clearly indicated that the total energy of form A is lower than that of form B for both DMBP-β-CD and DMAB-β-CD, so it could be concluded that form A would be the more stable species for the two compounds. It was found that the van der Waals energies of form A were lower than those of form B for DMAB-β-CD and DMBP-β-CD, (Figure 8(b) and 9(b)) indicating that the van der Waals energy difference between the A and B forms may be the primary factor for stabilizing form A. On the other hand, the angle bending energies of form A are higher than those of form B for DMAB-β-CD, indicating that the angle bending energy is a destabilizing factor for the formation of the self-inclusion complex. On the contrary, there is no variation of angle energies between the A and B forms for DMBP-β-CD, indicating there is no variation of angle energy upon formation of the self-inclusion complex. Since DMAB-β-CD has a stiff appending moiety, its CD ring must be distorted when DMAB-β-CD forms the self-inclusion complex. Consequently, the angle energy would be increased for DMAB-β-CD when it forms the self-inclusion complex. On the other hand, the appending moiety of DMBP-β-CD is flexible due to the presence of a trimethylene chain, DMBP-β-CD can form the self-inclusion complex without distortion of the CD ring, so there is no variation of angle energy upon formation of the self-inclusion complex. These calculated results were in good agreement with the experimental result, i.e., the population of the self-inclusion complex of DMBP-β-CD was larger than that of DMAB-β-CD.

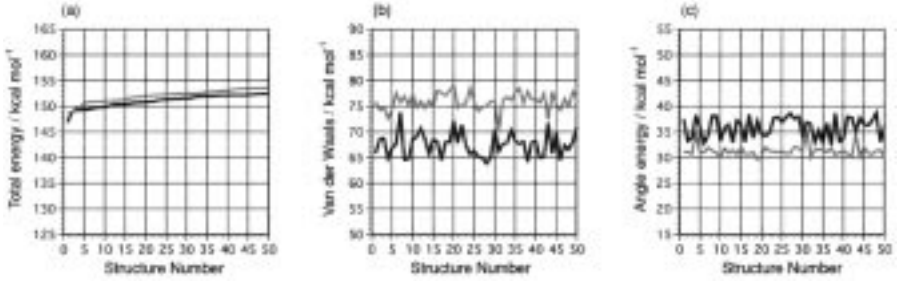

Figure 8. The total potential energy (a) of DMAB-β-CD calculated by MD conformational search (form A: ——; form B: ——). The component of total energy, i.e., (b) van der Waals energy and (c) angle bending energy are also shown (unit: kcal mol^{-1}).

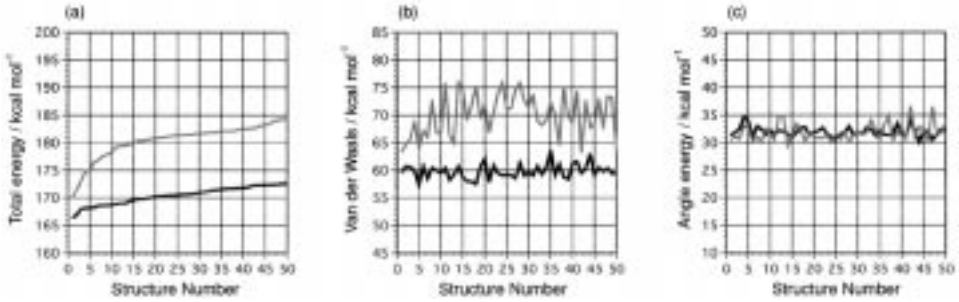

Figure 9. The total potential energy (a) of DMBP-β-CD calculated by MD conformational search (form A: ——; form B: ——). The component of total energy, i.e., (b) van der Waals energy and (c) angle bending energy are also shown (unit: kcal mol^{-1}).

4.2.3. *Enthalpy Difference between the A and B Forms*

Further analyses were performed with respect to the conformational equilibrium between the A and B forms to measure the enthalpy difference between the two forms. The difference in the Gibbs free energies between the two conformations (ΔG) were calculated from the fraction A_1 and A_2 using the Boltzman equation as shown below.

$$K = \frac{A_1}{A_2}$$

$$\Delta G = -RT \ln K$$

$$\ln K = \left(-\frac{\Delta H}{RT}\right) + \frac{\Delta S}{R}$$

where K is the equilibrium constant, ΔG is the free energy difference between the A and B forms, R is the gas constant, T is absolute temperature, ΔH is the enthalpy difference between the A and B forms and ΔS is the entropy difference between the A and B forms.

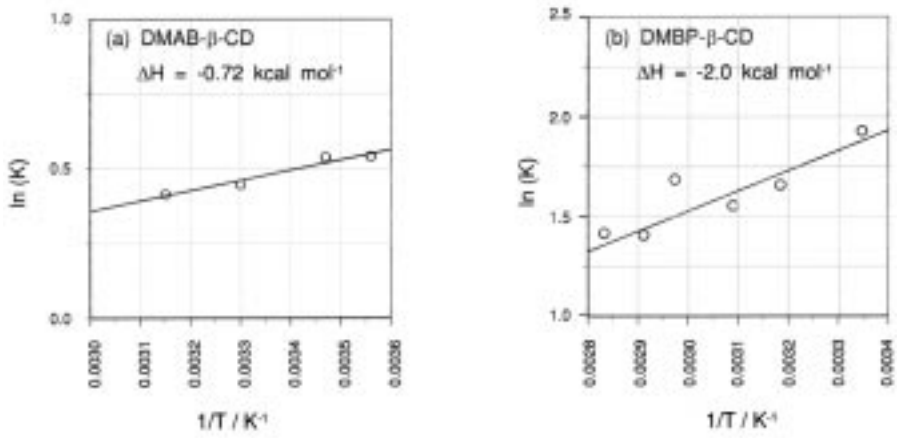

Figure 10. The plot of $\ln(K)$ vs. $1/T$ ((a) DMAB-β-CD and (b) DMBP-β-CD). The ΔH values were determined by a least-squares fitting procedure to the equation: $\ln(K) = (-\Delta H/RT) + (\Delta S/R)$ where R is the gas constant and T is the absolute temperature.

The K values were measured at various temperatures to determine some thermodynamic constants (ΔH). Table I and Table II show the calculated K and ΔG values. The plot of $1/T$ vs. $\ln(K)$ will give the ΔH and ΔS from the slope and the intercept, respectively (see Figure 10(a) and (b)).

In the case of DMAB-β-CD no (or a small) variation of K (equilibrium constant between the A and B forms) was observed at various temperatures, indicating that the value of ΔH is almost equal to 0 kcal mol^{-1} upon the formation of the self-inclusion complex (the calculated value of ΔH is -0.72 kcal mol^{-1}). On the other hand for DMBP-β-CD, a plot of $1/T$ vs. $\ln(K)$ gives a slope of a straight line, indicating that the ΔH in formation of the self-inclusion complex should have a negative value (ΔH is -2.0 kcal mol^{-1}). It was thus clearly demonstrated that the origin of the larger population of form A for DMBP-β-CD is the large gain of enthalpy upon formation of the self-inclusion complex, while the gain is small for DMAB-β-CD. In other words it can be concluded from the calculation that the gain of the van der Waals energy associated with self-inclusion of DMAB-β-CD is a primary factor for the negative value of ΔH. On the other hand, the gain of van der Waals energy in the formation of the self-inclusion complex invalidates the destabilization caused by increments of the angle bending energy, so the ΔH gained from the experiment almost equals zero. This is in good agreement with the calculated results, and indicates the validity of the calculated results.

5. Conclusion

The conformational analyses of modified CDs with a *p*-dimethylaminobenzene moiety were performed to investigate the conformational stability of the self-

inclusion complex. The spectroscopic analyses indicated that both DMAB-β-CD and DMBP-β-CD form self-inclusion complexes, and DMBP-β-CD, which has a flexible chain, has a larger population of the self-inclusion complex than DMAB-β-CD. On this basis, molecular dynamics conformational analyses were applied to the two modified CDs, DMAB-β-CD and DMBP-β-CD to clarify the reason why they have different trends in the stability of the self-inclusion complex. The computational analysis reveals that the self-inclusion structures of DMAB-β-CD and DMBP-β-CD are stabilized by van der Waals interaction between the appending moiety and the CD ring. In the case of DMAB-β-CD, the self-inclusion form is destabilized by increment of the angle energy, because the CD ring has to be distorted in including the DMAB moiety. On the other hand, there is no angle bending energy variation in forming the self-inclusion complex for DMBP-β-CD, because the flexible chain of the appending moiety allows formation of the self-inclusion complex without distortion of the CD ring. All these analyses demonstrate that the stability of the self-inclusion form depends on the appending moiety, especially the flexibility of the moiety.

Acknowledgment

This work was supported by Grant-in-Aid for Scientific Research from the Ministry of Education, Science, Culture, and Sports of Japan.

References

1. K. A. Connors: *Chem. Rev.* **97**, 1325 (1997).
2. K. Hamasaki, A. Nakamura, A. Ueno, and F. Toda: *Supramol. Chem.* **8**, 125 (1994).
3. T. Kuwabara, A. Nakamura, A. Ueno, and F. Toda: *J. Phys. Chem.* **98**, 6729 (1994).
4. A. Ueno, T. Kuwabara, A. Nakamura, and F. Toda: *Nature* **356**, 136 (1992).
5. K. Hamasaki, H. Ikeda, A. Nakamura, A. Ueno, and F. Toda: *J. Am. Chem. Soc.* **115**, 5035 (1993).
6. A. A. Bothner-By, R. L. Stephens, and J-m. Lee: *J. Am. Chem. Soc.* **106**, 811 (1984).
7. A. Bax and D. G. Davis: *J. Magn. Reson.* **63**, 207 (1985).
8. Y. Wang, T. Ikeda, A. Nakamura, H. Ikeda, A. Ueno, and F. Toda: *Bull. Chem. Soc. Jpn.* **67**, 1598 (1994).
9. R. A. Dunbar and F. V. Broght: *Supramol. Chem.* **3**, 93 (1994).
10. H. Ikeda, M. Nakamura, N. Ise, N. Oguma, A. Nakamura, T. Ikeda, F. Toda, and A. Ueno: *J. Am. Chem. Soc.* **118**, 10980 (1996).
11. P. M. Ivanov and C. Jamie: *J. Mol. Struct.* **377**, 137 (1996).
12. F. Perez, C. Jamie, and X. Sanchez-Ruiz: *J. Org. Chem.* **60**, 2740 (1995).
13. A. M. C. Myles, D. J. Barlow, G. France, and M. J. Lawrence: *Biochim. Biophys. Acta* **1199**, 27 (1994).
14. M. Fathallah, F. Fotiadu, and C. Jamie: *J. Org. Chem.* **59**, 1288 (1944).
15. F. Floegel and M. Mutter: *Biopolymer* **32**, 1283 (1992).
16. S. Usui, K. Hamasaki, T. Kuwabara, A. Nakamura, T. Ikeda, H. Ikeda, A. Ueno, and F. Toda: *Supramol. Chem.* **9**, 57–67 (1998).